

## Modifications of the Envelope of *Chlamydia psittaci* During Its Developmental Cycle: Freeze-Fracture Study of Complementary Replicas

CLAUDE LOUIS,<sup>1\*</sup> GISELE NICOLAS,<sup>2</sup> FRANÇOIS EB,<sup>3</sup> JEAN-FRANÇOIS LEFEBVRE,<sup>3</sup> AND JEANNE ORFILA<sup>3</sup>

*Station de Recherches de Pathologie Comparée INRA-CNRS, F 30380 Saint-Christol<sup>1</sup>; Laboratoire de Technologie Appliquée à la Microscopie Electronique, CNRS, F 75006 Paris<sup>2</sup>; and Laboratoire de Bactériologie, Faculté de Médecine, Université de Picardie, F 80036 Amiens,<sup>3</sup> France*

Examination of complementary replicas obtained by freeze-fracture of *Chlamydia psittaci* revealed, at the level of the plasma membrane, a progressive differentiation of "crater-like formations," which likely correspond to transmembranal pores. Recognition of "early" and "late" stages observed in the intermediate bodies permitted detailed study of the developmental cycle of this chlamydia.

Chlamydiae are obligate intracellular procarotes, for which Storz and Page created the order *Chlamydiales* (25). They are characterized by a developmental cycle occurring within cytoplasmic vacuoles (5-7, 11, 12, 20, 21).

Many studies were carried out on the *Chlamydia* envelope (for review, see Becker [1]). In an electron microscopic study of purified cell walls, Manire (16) reported hexagonally arrayed structures, which were later confirmed by several authors (9, 17, 19, 21, 24). Based on a freeze-etching technique without double replicas, Kajima et al. (10) and Matsumoto (17) reported studies on *Chlamydia trachomatis* and *Chlamydia psittaci*, respectively. Matsumoto also showed, by freeze-etching, hexagonally arrayed structures. The relationship between these two types of structures is not yet defined clearly.

Using the freeze-fracture technique with complementary replicas obtained in ultrahigh vacuum and at very low temperature, we obtained new data on the modification of the *C. psittaci* envelope appearing during the chlamydial cycle.

### MATERIALS AND METHODS

**Chlamydial strain and cell cultures.** The Loth ornithosis strain of *C. psittaci* was used in this study. This strain was multiplied in HeLa 229 or in L929 cell lines and infected as previously described by Popov et al. (21).

**Electron microscopy.** Fixations were carried out when 80% of the cells were infected. Glutaraldehyde (2.5%) in 0.1 M cacodylate buffer (pH 7.2) was added at 37°C for 1 h. The flask was rinsed with the cacodylate buffer at laboratory temperature, and the cells were gently scraped. The cells were sedimented by low-speed centrifugation, and the pellet was impregnated with 25% glycerol for 20 to 30 min to avoid ice-crystal formation. These samples were again centri-

fuged, and then were sandwiched between two specimen holder dishes 3 mm in diameter for double-replica technique. They were then fractured in a Cryofract device by the method of Escaig and Nicolas (8), and both complementary fractures were shadowed by platinum evaporation. The replicas were cleaned in sodium hypochlorite, rinsed in double distilled water, dried, and examined in a transmission electron microscope at 75 kV. For control, thin sections of cells were postfixed in osmium tetroxide, dehydrated, and embedded in polyester resins.

### RESULTS

Complementary cleavages obtained by freeze-fracturing enabled us to examine and compare the opposite structures of both the concave and the convex faces of the same material.

**Host cells.** The fractured cells clearly showed the cleavage surface of the plasma membranes, the inner and outer membranes of mitochondria, the numerous vacuolar membranes, and, occasionally, the ergastoplasmic reticulum.

The vacuoles filled with chlamydiae were surrounded by a membrane whose convex face was almost entirely smooth (Fig. 1, EV). The opposite concave face showed numerous particles (Fig. 2, PV). The fractured surface of the vacuolar material lying between the chlamydiae was almost smooth.

**The microorganisms.** On ultrathin sections, the various developmental stages were observed (Fig. 3). The bodies were spherical in shape, surrounded by a plasma membrane that was often difficult to observe (12) and by a cell wall whose outer membrane was also trilamellar in structure. As previously described, the reticulate bodies (RB) were 0.6 to 1  $\mu$ m in size. By reduction of their size and by differentiation of a

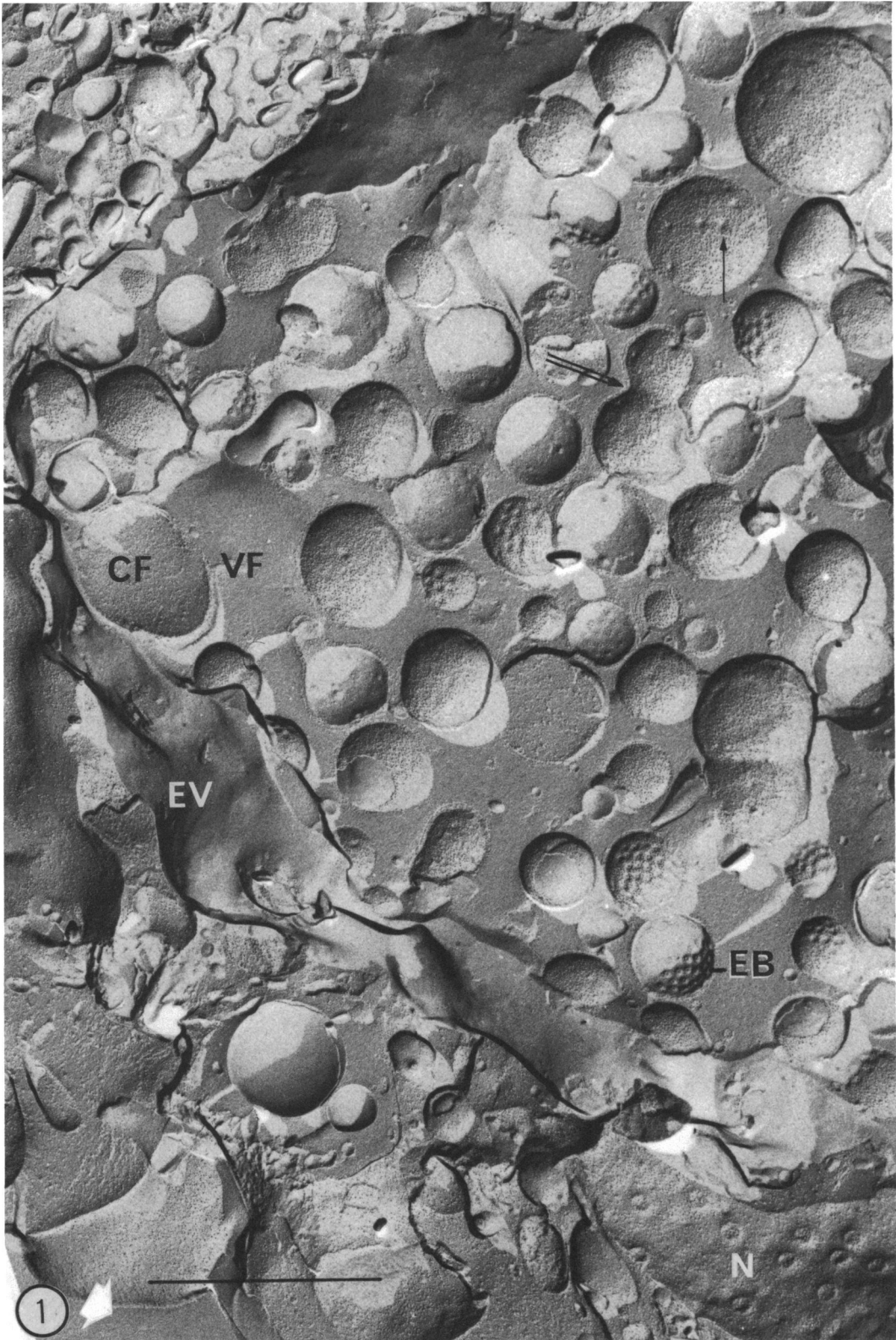


**FIG. 1 and 2.** Complementary replicas of a microcolony of *C. psittaci* in an L929 cell. N, Host cell nucleus; PV and EV, P and E faces of the vacuolar membrane enclosing the chlamydiae; VF, vacuolar fluid; CF, transversal fracture of a reticulate body; EB (see also Fig. 5 and 6) with craters. Single arrow, Incomplete crater; double arrow, constriction suggesting a process of division. Bar, 1  $\mu$ m;  $\times 36,000$ . Arrows at bottom indicate the direction of shadowing.

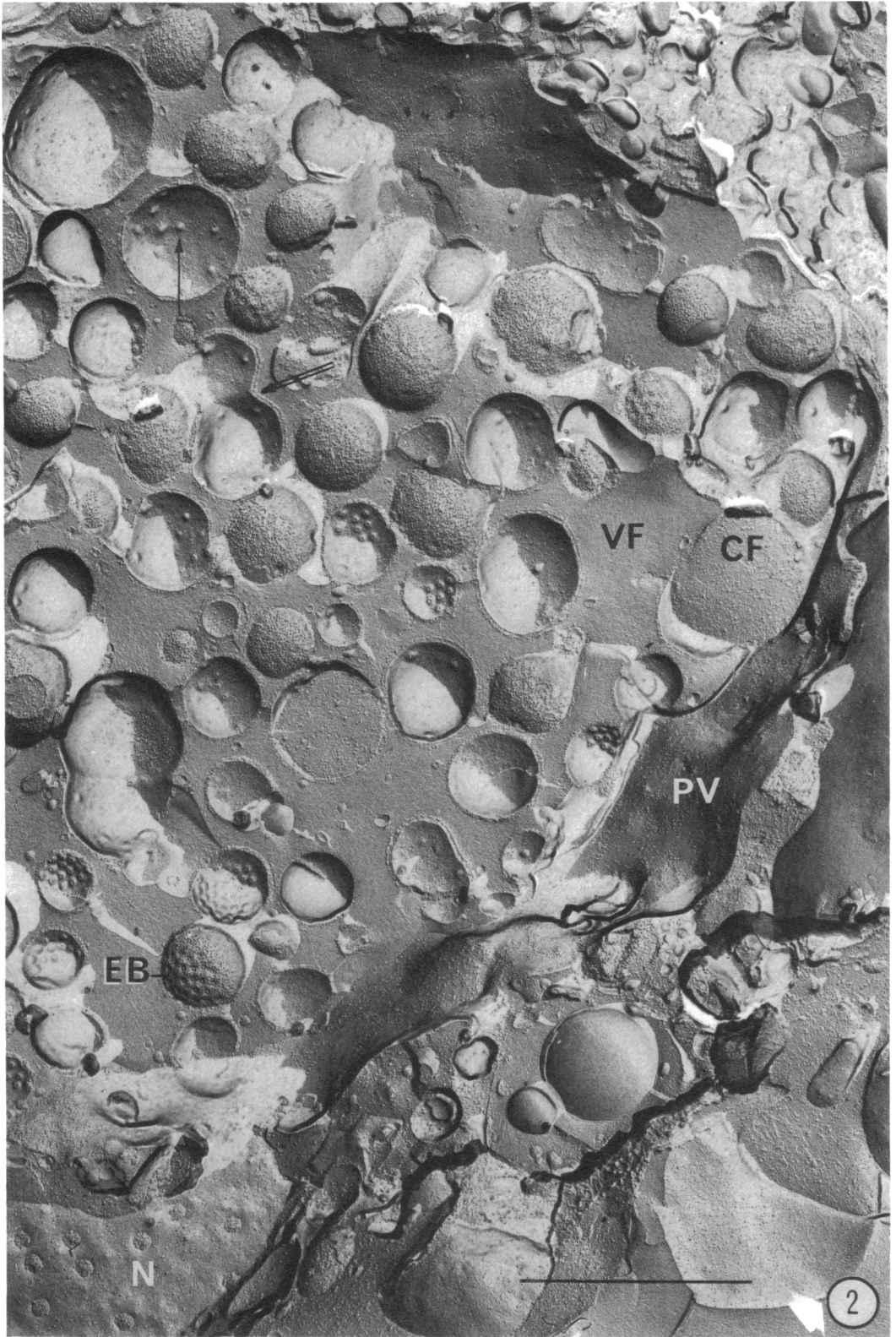


FIG. 2  
870

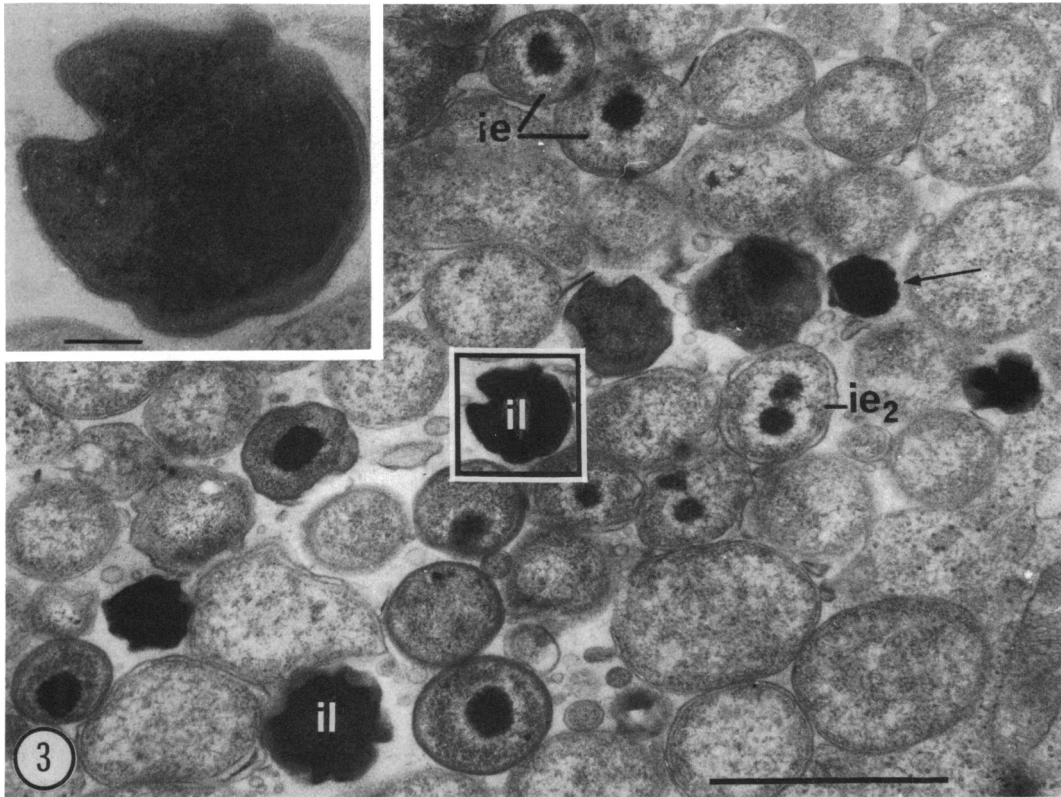


FIG. 3. Microcolony of *C. psittaci* in L929 cells. Ultrathin section. Arrow: EB with hemispheric projections; *ie*, early type of IB with a differentiated nucleoid; *ie*<sub>2</sub>, the same, with two nucleoids; *il*, late type of IB (see also insert). Bar, 1  $\mu$ m;  $\times 31,000$ . Insert: bar, 0.1  $\mu$ m;  $\times 105,000$ .

nucleoid, they became transformed into intermediate bodies (IB) and finally into elementary bodies (EB), small dense forms of approximately 0.3  $\mu$ m in diameter, with a sublateral nucleoid. Concerning more specifically the IB, we were able to observe two main types (Fig. 3). Some were still similar to RB, with a spherical shape, an electron-clear cytoplasm, and a smooth envelope, but they differed from RB by a dense simple or multiple nucleoid. They were 0.6 to 0.45  $\mu$ m in size and might be able to undergo division. Others with an average diameter of 0.45  $\mu$ m presented a dense sublateral nucleoid, a cytoplasm at different stages of densification, and projections of the envelope (Fig. 3 and insert). We consider these second forms as a further step of differentiation just preceding the EB, which often possess hemispheric surface projections (Fig. 3) similar to those observed by several authors (9, 18, 21, 24).

Freeze-fracture of RB showed two different cleavage zones (CZ), an inner one and an outer one (Fig. 1, 2, and 4). The inner CZ was covered

on its convex face by numerous particles, whereas the opposite concave face was almost smooth with only a few particles per square micrometer. The outer CZ was less frequently observed. It was almost smooth on its convex face. The concave face showed smooth areas and irregularly distributed granular areas. RB were sometimes observed in the process of elongation and constriction.

Freeze-fracture of EB (Fig. 1, 2, 5, and 6) showed only one CZ, with numerous particles covering the convex face, whereas the concave face possessed very few particles. The complementary structure of both faces is clearly shown in Fig. 5 and 6. This membrane showed peculiar "crater-like formations," constituted on the concave face by protrusions of approximately 30 to 40 nm in diameter. A 14- to 20-nm depression showing a small (3- to 6-nm) knob was located in the center. The convex face presented depressions of the same diameter as the craters of the concave face, with a centrally positioned circular protrusion 14 to 20 nm in diameter showing a



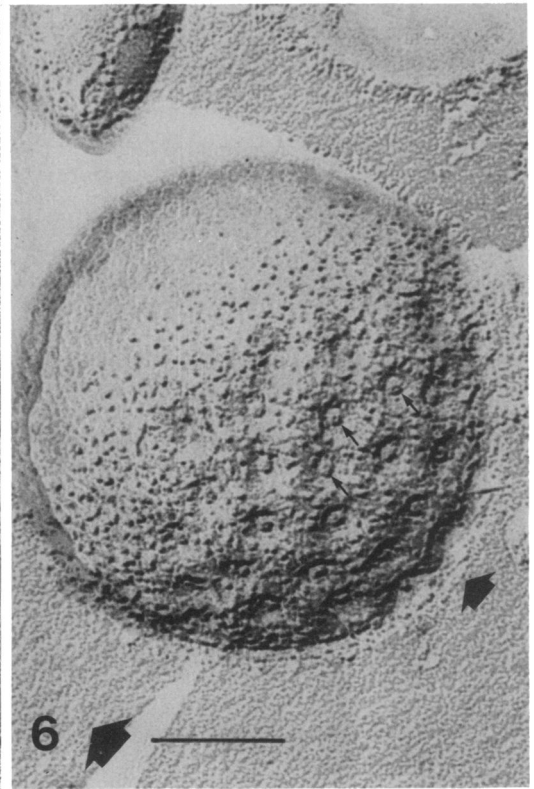
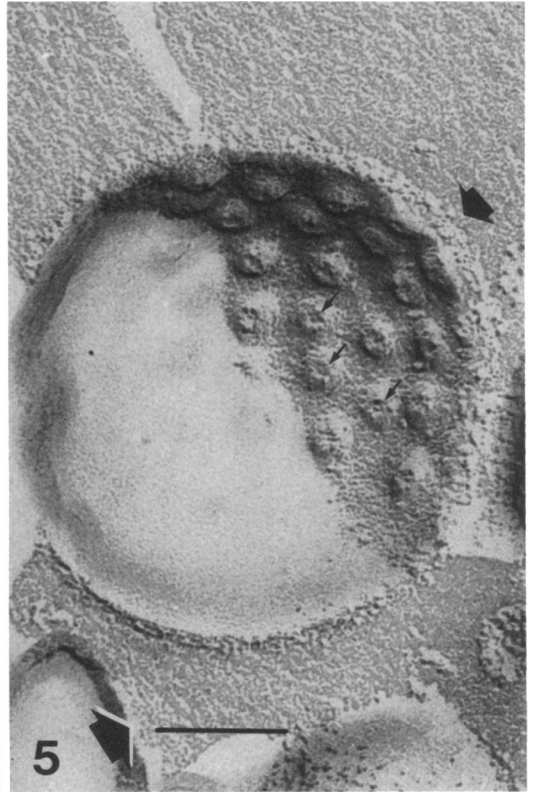


**FIG. 4.** Cell wall cleavage of the outer membrane of RB (arrows). Thin arrow, Convex face, almost smooth; wide arrow, concave face, partially smooth with some granules. Bar, 1  $\mu\text{m}$ ;  $\times 60,000$ . Arrow at bottom left indicates direction of shadowing.

**FIG. 5 and 6.** Enlargements of the complementary replicas of Fig. 1 and 2. Cleavage of the plasma membrane of an EB: Fig. 5, E face; Fig. 6, P face. Thin arrows: Porelike structures in the center of the craters, seen as small pits on the P face and small knobs on the E face. Wide arrows: Transversal fractures of the cell wall. Bar, 0.1  $\mu\text{m}$ ;  $\times 170,000$ . Arrows at bottom left indicate direction of shadowing.

small (3- to 6-nm) hollow in its center. These structures were arrayed in hexagonal arrangements.

We did not succeed in observing any outer CZ in EB in spite of our efforts to visualize it by postfixing the samples in different conditions and by fracturing at several temperatures or without glycerol. Similarly, we failed to observe "projections" on transversal fractures of the outer zone, whose surface appeared almost smooth (Fig. 5 and 6).

Some bodies, about 0.45  $\mu\text{m}$  in diameter, showed craters similar to those observed in EB. According to their size and structure, these forms should be considered IB (Fig. 7). Sometimes, the craters, not entirely differentiated, were devoid of the central granule (Fig. 1 and 2, single arrows). These bodies occasionally showed a transversal constriction, suggesting a process of division (Fig. 1 and 2, double arrows).

### DISCUSSION

The complementary replicas we obtained enabled us to present data and interpretations in accordance with the present knowledge of the cleavage mechanism of the biological membranes of eucaryotic and procaryotic cells, particularly gram-negative bacteria (2-4, 13, 22, 26, 27) and chlamydia-like rickettsias of invertebrates (14, 15).

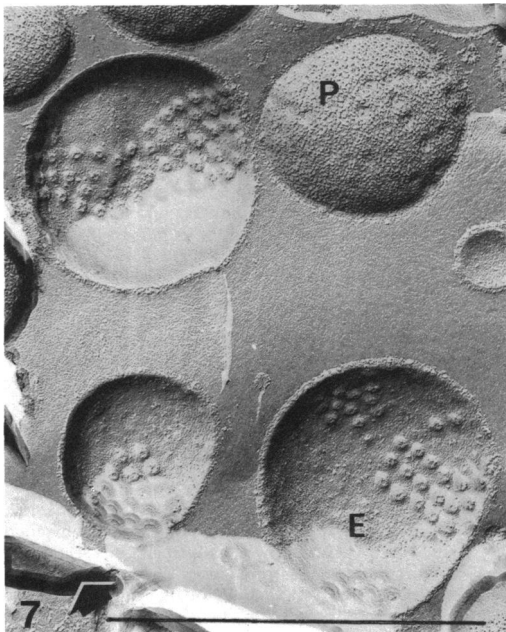


FIG. 7. Freeze-fracture of the plasma membrane of IB, showing the craters. P, P face; E, E face. Bar, 1  $\mu\text{m}$ ;  $\times 50,000$ . Arrow at bottom left indicates direction of shadowing.

The CZ of the host cell membrane shows, according to Branton et al. (3), the plasmic "P" face with numerous particles and the external "E" face with rare particles.

The inner CZ appearing in the RB clearly occurred at the level of the plasma membrane. Indeed, the convex face with numerous particles may be assimilated to the P face, and the opposite one may be assimilated to the E face. The outer CZ of the RB corresponded to the outer membrane of the bacterial cell wall. The convex face with a smooth surface was not significantly different from the corresponding face in most of bacteria. However, the structure of the concave face, with only a few granules, resembled more that of a rickettsia pathogenic for the scorpion *Buthus occitanus* (14) than the concave face of the cell wall of gram-negative bacteria and of some rickettsiae (14, 15), where many granules have been described. Membrane cleavage was observed by Kajima et al. and by Matsumoto (10, 17) but interpreted differently. The cell wall cleavage was not observed.

In EB, the only CZ was characteristic of the plasma membrane with convex P and concave E faces. The numerous craters were apparently limited to a hemisphere; this location could be related to the eccentric position of the nucleoid. The granule located in the center of the crater cavity of the P face was wider than the usual particles of the plasma membrane. The small central hollow, several nanometers in diameter, observed in the middle of this granule likely corresponded to a small canal, its complementary structure appearing as a little knob on the E face. No cell wall cleavage could be detected in EB; this very likely resulted from important reorganizations occurring in the structure of the outer membrane. The craters of EB, called buttons by Matsumoto (17), were previously observed but with a less sophisticated interpretation of their structure and of the mechanism of freeze-fracture.

According to their structure on ultrathin sections, two main types of IB could be distinguished. The first type, with a spherical shape, an electron-clear cytoplasm, and a centrally located nucleoid, would represent an "early" IB, still able to undergo division. The second type, with projections of the envelope, an electron-dense cytoplasm, and an eccentric nucleoid, could represent a "late" IB in an advanced stage of condensation, likely corresponding to the IB that showed well-differentiated craters by freeze-fracture. Incomplete craters could start differentiating at the early stage of IB or even at the stage of RB. Until now, the cleavage and craters of IB have not been observed.

Moreover, the craters of the plasma mem-

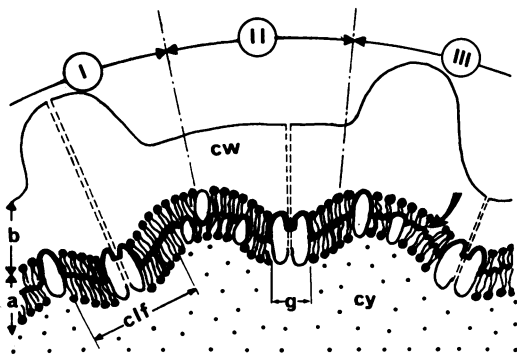


FIG. 8. Diagrammatic representation of a transversal section of the EB envelope. Zone a, Plasma membrane. Three crater-like formations next to each other are illustrated (clf). The phospholipid bilayer and the membrane proteins are schematized according to the fluid mosaic model of Singer and Nicolson (23). The central granule of the craters (g) is represented as a molecule crossed by a canal continuing through the cell wall. Cleavage zone: Wide line (curved arrow). Zone b, Cell wall (cw). The surface is supposed to be either smooth (II) or bearing hemispheric surface projections located above craters (I) or between adjacent craters (III).

brane could be in relation to the hemispheric surface projections of the cell wall (shown in Fig. 3 and previously described by several authors [9, 16, 17, 19, 21, 24]), whose role in attachment to host cells is controversial (9). Both types of formations show a similar hexagonal arrangement (16, 17), but we have no data to define whether they are superimposed or not. In our studies, we failed to observe any projections on transverse fractures of the cell wall (Fig. 5 and 6). It is thus possible that they are appearing only at a given physiological stage or as a result of external conditions. The three possibilities concerning the relations between the craters and the cell wall are illustrated schematically in Fig. 8.

As mentioned above, if a canal is crossing the central granule of craters, these formations might represent transmembranous pores of a peculiar nature. They could play a role in the transfer of substances at different stages of the cycle, especially during the process of condensation of late IB or the swelling of EB.

#### ACKNOWLEDGMENT

We thank G. Kuhl for skillful technical assistance.

#### LITERATURE CITED

1. Becker, Y. 1978. The chlamydia: molecular biology of prokaryotic obligate parasites of eucaryocytes. *Microbiol. Rev.* **42**:274-304.
2. Branton, D. 1966. Fracture faces of frozen membranes. *Proc. Natl. Acad. Sci. U.S.A.* **55**:1048-1056.
3. Branton, D., S. Bullivant, N. B. Gilula, M. J. Karnovsky, H. Moor, K. Muelhenthaler, D. H. Northcote, L. Packer, B. Satir, P. Satir, V. Speth, L. A. Staehlin, R. L. Steere, and R. S. Weinstein. 1975. Freeze etching nomenclature. *Science* **190**:54-56.
4. Costerton, J. W., J. M. Ingram, and K. J. Cheng. 1974. Structure and function of the cell envelope of gram-negative bacteria. *Bacteriol. Rev.* **38**:87-110.
5. Costerton, J. W., L. Poffenroth, J. C. Wilt, and N. Kordova. 1976. Ultrastructural studies of the nucleoids of the pleomorphic forms of *Chlamydia psittaci* 6 BC: a comparison with bacteria. *Can. J. Microbiol.* **22**:16-28.
6. Devauchelle, G., C. Vago, and G. Meynadier. 1971. Ultrastructure comparée de *Rickettsiella melolonthae* (Rickettsiales, Wolbachiae) et de l'agent de la lymphogranulomatosse vénérienne (Rickettsiales, Chlamydiaceae). *C.R. Acad. Sci. Paris* **272**:2972-2974.
7. Eb, F., G. Devauchelle, and J. Orfila. 1972. Etude ultrastructurale de l'agent de la lymphogranulomatosse vénérienne (Rickettsiales, Chlamydiaceae). *J. Microsc. (Paris)* **13**:47-56.
8. Escaig, J., and G. Nicolas. 1976. Cryo-fractures de matériel biologique réalisées à très basses températures en ultra-vide. *C.R. Acad. Sci. Paris* **283**:1245-1248.
9. Gregory, W. W., M. Gardner, G. I. Byrne, and J. W. Moulder. 1979. Arrays of hemispheric surface projections on *Chlamydia psittaci* and *Chlamydia trachomatis* observed by scanning electron microscopy. *J. Bacteriol.* **138**:241-244.
10. Kajima, M., H. Miyamoto, and Y. Mitsui. 1973. Fine structure of trachoma agent as observed by freeze-etching electron microscopy. *Acta Soc. Ophthalmol. Jpn.* **77**:1184-1193.
11. Lepinay, A., J. Orfila, A. Anteunis, J. M. Boutry, L. Orme-Rosselli, and R. Robineaux. 1970. Etude en microscopie électronique du développement et de la morphologie de l'agent de l'ornithose dans les macrophages de souris. *Ann. Inst. Pasteur* **119**:222-231.
12. Lepinay, A., H. Robineaux, J. Orfila, L. Orme-Rosselli, and J. M. Boutry. 1971. Ultrastructure and cytochemistry of *Chlamydia psittaci*. *Arch. Gesamte Virusforsch.* **33**:271-280.
13. Li, J. K. K., and C. F. Fox. 1975. Ultrastructural studies on the inner and outer membranes of an unsaturated fatty acid auxotroph of *Escherichia coli*. *J. Ultrastruct. Res.* **52**:120-133.
14. Louis, C., G. Morel, G. Nicolas, and G. Kuhl. 1979. Etude comparée des caractères ultrastructuraux de rickettsies d'arthropodes, révélés par cryodécoupage et cytochimie. *J. Ultrastruct. Res.* **66**:243-253.
15. Louis, C., A. Yousfi, C. Vago, and G. Nicolas. 1977. Etude par cytochimie et cryodécoupage de l'ultrastructure d'une *Rickettsiella* de Crustacé. *Ann. Microbiol. (Inst. Pasteur)* **1288**:177-205.
16. Manire, G. P. 1966. Structure of purified cell walls of dense forms of meningopneumonitis organisms. *J. Bacteriol.* **91**:409-413.
17. Matsumoto, A. 1973. Fine structures of cell envelopes of *Chlamydia* organisms as revealed by freeze-etching and negative staining techniques. *J. Bacteriol.* **116**:1355-1363.
18. Matsumoto, A., E. Fujikawara, and N. Higashi. 1976. Observations on the surface projections of infectious small cells of *Chlamydia psittaci* in thin sections. *J. Electron Microsc. Res.* **25**:169-170.
19. Matsumoto, A., and G. P. Manire. 1970. Electron microscopic observations on the fine structure of cell walls of *Chlamydia psittaci*. *J. Bacteriol.* **104**:1332-1337.
20. Page, L. A. 1971. Order *Chlamydiales* Storz and Page, 334, p. 915-925. In R. E. Buchanan and N. E. Gibbons (ed.), *Bergey's manual of determinative bacteriology*, 8th ed. The Williams and Wilkins Co., Baltimore.
21. Popov, V., F. Eb, J. F. Lefebvre, J. Orfila, and A.

- Viron.** 1978. Morphological and cytochemical study of *Chlamydia* with EDTA regressive technique and Gaudier staining in ultrathin frozen sections of infected cell cultures: a comparison with embedded material. *Ann. Microbiol. (Inst. Pasteur)* **129**:313-337.
22. **Salton, M. R. J., and P. Owen.** 1976. Bacterial membrane structure. *Annu. Rev. Microbiol.* **30**:451-482.
23. **Singer, S. J., and G. L. Nicolson.** 1972. The fluid mosaic model of the structure of cell membranes. *Science* **175**:720-731.
24. **Stokes, G. V.** 1978. Surface projections and internal structure of *Chlamydia psittaci*. *J. Bacteriol.* **133**:1514-1516.
25. **Storz, J., and L. A. Page.** 1971. Taxonomy of the Chlamydiae: reasons for classifying organisms of the genus *Chlamydia*, family *Chlamydiaceae*, in a separate order, *Chlamydiales* ord. nov. *Int. J. Syst. Bacteriol.* **21**:332-334.
26. **Thornley, M. J., and U. B. Sleytr.** 1974. Freeze etching of the outer membranes of *Pseudomonas* and *Acinetobacter*. *Arch. Microbiol.* **100**:409-417.
27. **Van Gool, A. P., and N. Nanninga.** 1971. Fracture faces in the cell envelopes of *Escherichia coli*. *J. Bacteriol.* **108**:474-481.